Computational Study on the Relative Reactivities of Cobalt and Nickel Amidinates via β-H Migration

Jinping Wu,*,† Jiaye Li,† Chenggang Zhou,† Xinjian Lei,‡ Thomas Gaffney,‡ John A. T. Norman,‡ Zhengwen Li,§ Roy Gordon,§ and Hansong Cheng*,||

Institute of Theoretical Chemistry and Computational Materials Science, China University of Geosciences, Wuhan, People's Republic of China 430074, Air Products and Chemicals, Inc., 1969 Palomar Oaks Way, Carlsbad, California 92011, Department of Chemistry and Chemical Biology, Harvard University, Cambridge, Massachusetts 02138, and Air Products and Chemicals, Inc., 7201 Hamilton Boulevard, Allentown, Pennsylvania 18195

Received October 4, 2006

Summary: Density functional theory calculations were performed to examine the relative stabilities of several Co- and Ni-based amidinates for atomic layer deposition to β-H or β-CH_3 migration from the chelating ligand to the metal center atom. The calculated precursor structures are in excellent agreement with the available XRD data. The minimum energy path of the migration process was identified. Our results indicate that the migration process is thermochemically endothermic; however, for Ni(^{i}Pr-MeAMD)$_2$ the reaction is close to thermoneutral. The relatively moderate activation barrier allows β-H migration for Ni(^{i}Pr-MeAMD)$_2$ to occur, leading to instability at the ALD process temperature. Replacing the H atoms with methyl groups can greatly stabilize the precursors to the β-H migration. The results are consistent with the experimental observations.

As the feature size of semiconductor devices continues to shrink,[1] atomic layer deposition (ALD) has become the preferred technique to deposit extremely thin, conforming metal films on surfaces of partially fabricated semiconductor substrates, such as W, Ta, and transition-metal nitrides.[2−4] The design and development of sufficiently stable metal-organic precursors is of great interest for ensuring successful ALD applications. Recently, Gordon et al.[5] synthesized a number of novel amidinates as ALD precursors for deposition of cobalt thin films on ALD WN as a glue layer for copper interconnects, or nickel and cobalt thin films on silicon surfaces for fabrication of NiSi and $CoSi_2$ as the contact metals in micro- and nanoelectronics.[6,7] The amidinate ligands in the precursors are chelating *N*,*N*′-diisopropylacetamidinato and *N*,*N*′-di-*tert*-butylacetamidinato ligands. It was found that bis(*N*,*N*′-diisopropylacetamidinato)-nickel(II) (Ni(^{i}Pr-MeAMD)$_2$) is thermally less stable than bis-(*N*,*N*′-di-*tert*-butylacetamidinato)nickel(II) (Ni(^{t}Bu-MeAMD)$_2$), whereas both bis(*N*,*N*′-diisopropylacetamidinato)cobalt(II) (Co(^{i}Pr-MeAMD)$_2$) and bis(*N*,*N*′-di-*tert*-butylacetamidinato)-cobalt(II) (Co(^{t}Bu-MeAMD)$_2$) are stable.[8,9] It was thus speculated that the migration of one of the β-H atoms from the bis(*N*,*N*′-diisopropylacetamidinato) ligands to the metal atom could be related to the thermal degradation of the precursor. β-H migration has been observed in many organometallic reactions.[10−13] However, why the degradation occurs more readily in Ni(^{i}Pr-MeAMD)$_2$ than in Co(^{i}Pr-MeAMD)$_2$ remains to be addressed. The purpose of this communication is to examine quantitatively the decomposition mechanism arising from the β-H migration by computing the thermochemical energies and reaction pathways using density functional theory (DFT). The results might provide useful insight into the relative reactivity and thermal stability of the ALD precursors and should aid the design of novel precursors in the future.

All calculations were performed under the generalized gradients approximation (GGA) with the Perdew−Wang exchange-correlation functional (PW91) as implemented in the DMol^3 package.[14,15] The spin-polarization scheme was employed to deal with the electronic open-shell systems. A double numerical atomic basis set augmented with polarization functions (DNP) was used to describe the valence electrons, and the core electrons were represented by effective core potentials (ECP). All-electron (AE) calculations using the DNP basis set were also performed for selected precursors, and the difference in the calculated structures and energetics between ECP and AE calculations was found to be relatively small. Full geometry optimization was performed for all of the reactants and products. The transition state search employed the protocol of complete linear synchronous transit/quadratic synchronous transit (LST/QST), and the transition state optimization utilized the Newton−Raphson search algorithm. Normal-mode analysis was conducted to ensure the correctness of the obtained transition states.

The reaction pathway is schematically shown as reactant, transition state, and product in Figure 1, where R represents the migrating species (R = H if the ligand is bis(*N*,*N*′-

* To whom correspondence should be addressed. E-mail: chengh@airproducts.com H.C.); jpwu@cug.edu.cn (J.W.)
† China University of Geosciences.
‡ Air Products and Chemicals, Inc., Carlsbad, CA.
§ Harvard University.
|| Air Products and Chemicals, Inc., Allentown, PA.

(1) Moore, G. *Electronics* **1965**, *38*(8).
(2) Becker, J. S.; Suh, S.; Wang, S.; Gordon, R. G. *Chem. Mater.* **2003**, *15*, 2969.
(3) Park, K.-H.; Marshall, W. J. *J. Am. Chem. Soc.* **2005**, *127*, 9330.
(4) Kim, H. *J. Vac. Sci. Technol., B* **2003**, *21*(6), 2231−2261.
(5) Booyong, S. L.; Rahtu, A.; Gordon, R. G. *Nat. Mater.* **2003**, *2*, 749.
(6) Zhang, S.; Ostling, M. *Crit. Rev. Solid State Mater. Sci.* **2003**, *28* (1), 1.
(7) Wu, Y.; Xiang, J.; Yang, C.; Lu, W.; Lieber, C. M. *Nature* **2004**, *430* (61), 6.
(8) Li, Z.; Gordon, R. G.; Farmer, D. B.; Lin, Y.; Vlassak, J. *Electrochem. Solid-State Lett.* **2005**, *8*(7), G182.
(9) Gordon, R. G.; Lim, B. S. Atomic Layer Deposition using Metal Amidinates. PCT Int. Patent WO 2004046417, 2004.
(10) Mole, L.; Spencer, J. L.; Carr, N.; Orpen, A. G. *Organometallics* **1991**, *10*, 49−52.
(11) Hartwig, J. F.; Bergman, R. G.; Andersen, R. A. *Organometallics* **1991**, *10*, 3326.
(12) Brookhart, M.; Hauptman, E.; Lincoln, D. M. *J. Am. Chem. Soc.* **1992**, *114*, 10394.
(13) Doherty, S.; Hogarth, G.; Waugh, M.; Clegg, W.; Elsegood, M. R. J. *Organometallics* **2000**, *19*, 4557.
(14) Perdew, J. P.; Wang, Y. *Phys. Rev. B* **1992**, *45*(13), 244.
(15) Delley, B. *J. Chem. Phys.* **2000**, *113*(18), 7756−7764.

10.1021/om060910a CCC: $37.00
Publication on Web 04/21/2007

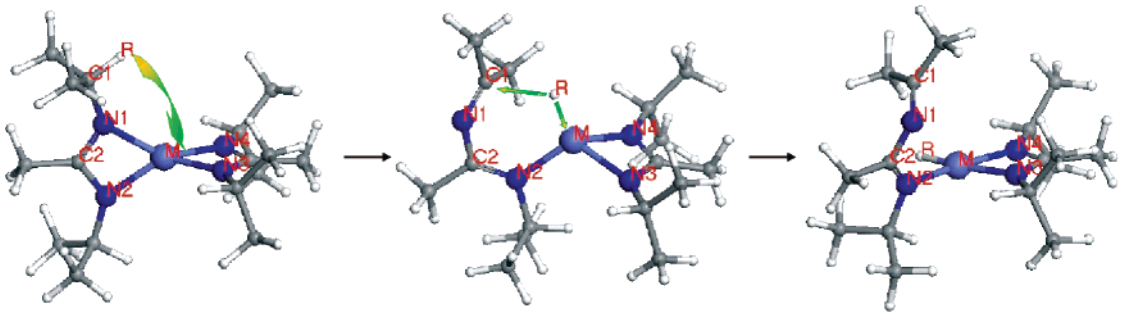

Figure 1. Structures of the reactant, transition state, and product: M = Ni, Co and R = H, CH_3.

Table 1. Main Optimized Precursor Structural Parameters and Comparison with the Available Experimental Data

	^{i}Pr-MeAMD		^{t}Bu-MeAMD	
	Co exptl/ calcd	Ni calcd	Co calcd	Ni exptl/ calcd
M−N1 (Å)	2.004/2.017	2.011	2.021	1.991/2.013
M−N2 (Å)	2.020/2.030	2.021	2.037	1.997/2.021
M−N3 (Å)	2.004/2.032	2.021	2.037	1.991/2.026
M−N4 (Å)	2.020/2.016	2.013	2.024	1.997/2.013
C1−N1 (Å)	1.447/1.461	1.458	1.470	1.466/1.466
C2−N1 (Å)	1.322/1.342	1.338	1.343	1.335/1.339
C2−N2 (Å)	1.318/1.342	1.339	1.341	1.318/1.341
N1−M−N2 (deg)	65.57/65.65	65.94	65.60	66.20/65.87
N3−M−N4 (deg)	65.57/65.69	65.91	65.55	66.20/65.76
N1−N2−N3−N4 (deg)	80.58/83.58	83.77	83.95	82.18/83.90

Table 2. Calculated Rotational Barriers and Rotational Energies of Co(^{i}Pr-MeAMD)$_2$ and Ni(^{i}Pr-MeAMD)$_2$ Precursors (kcal/mol)[a]

precursor	rotational barrier	rotational energy
Co(^{i}Pr-MeAMD)$_2$	1.5	3.6
Ni(^{i}Pr-MeAMD)$_2$	1.0	6.5

[a] The rotational energy is defined as the energy difference of isomers upon internal rotation.

diisopropylacetamidinato) and R = CH_3 if the ligand is bis-(*N*,*N*′-di-*tert*-butylacetamidinato)). M represents Ni or Co. The main geometric parameters of the fully optimized precursor structures and a comparison with the available experimental data are shown in Table 1. Structural information on transition states and final products is given in the Supporting Information. The minimum-energy structure of the reactants adopts a distorted-tetrahedral framework, with the dihedral angles formed by four nitrogen atoms around the center metal atom being 83.6° and 83.8° for Co(^{i}Pr-MeAMD)$_2$ and Ni(^{i}Pr-MeAMD)$_2$, respectively, reflecting the steric effect on the backbone. The calculated reactant structures are in excellent agreement with the XRD results.[16] We note that there is partial electron delocalization among the N−C−N atoms of the two four-membered rings, which results in relatively weak coordination between N atoms and the metal. The R groups on the isopropyl groups of the reactants are out of the plane formed by the four-membered rings. For one of the R groups, R1, to migrate from the C1 to the metal center, it is necessary for the isopropyl group to undergo an internal rotation to align it with the four-membered ring in the same plane to minimize the migration barriers. Indeed, this can be readily realized under ambient conditions, since our calculations indicate that the internal rotation results in an energy barrier of only a few kcal/mol, consistent with the XRD experiments. The calculated internal rotation barriers are shown in Table 2.

Upon R1 group migration, the N1−M bond of the products becomes significantly elongated and the C1−N1 bond simultaneously evolves into a double bond; a strong single R1−M bond is also formed. The strain imposed by the four-membered ring is relaxed upon the N1−M bond breaking. As a consequence, the metal centers of the products adopt a square configuration.

The optimized transition state geometries for both Ni and Co precursors are quite similar, although the structural details differ. Essentially, the R1 group resides between C1 and M, forming two rather loose single bonds. For R1 = CH_3, the C1 atom is repelled farther away from the metal atom due to steric effects.

The change of geometric structures along the migration pathway gives rise to a significant change of electronic structures of the reactants, products, and transition states. The reactants all adopt a high-spin state for both R = H and R = CH_3 due to the weak coordination of the ligand field. For the Ni precursors, there are two unpaired electrons occupying HOMO and HOMO1, while for the Co precursors, there are three unpaired electrons in the low-lying orbitals. Upon R1 group migration, a strong R1−M bond is formed and the change of metal electronic configuration from tetrahedral to square gives rise to a low-spin state for the products. Indeed, the calculated ground electronic state of the products yields only one unpaired electron on Co and zero on Ni. At the transition states, the poor coordination gives both compounds a high-spin state, the same as for the reactants. The change of the high-spin states of transition states to the low-spin states of products indicates crossing of potential energy surfaces. Indeed, our minimum energy pathway calculations for both high-spin and low-spin states of Co(^{i}Pr-MeAMD)$_2$ and Ni(^{i}Pr-MeAMD)$_2$ show that curve crossing occurs near the vicinity of the transition states (Figure 2), after which the potential energies decrease rapidly along the low-spin-state pathways. The calculated structures at the crossing points are shown in the Supporting Information. It is interesting that the potential energies of the high-spin states are nearly flat after the transition states. The electronic configuration of the optimized final products for both Ni and Co of the high-spin states is a distorted tetrahedron, while for the low-spin-state products the electronic configuration changes to a square. The ligand−metal coordination is also considerably weakened for the high-spin-state products, with the elongations of the N−M and H−M bond distances being about 0.16 and 0.09 Å for Ni(^{i}Pr-MeAMD)$_2$ and 0.11 and 0.04 Å for Co(^{i}Pr-MeAMD)$_2$, respectively.

To understand the relative stability, we first consider R = H. The calculated thermochemical energies and the activation barriers for the Ni and Co precursors are shown in Table 3. The results of our calculations indicate that thermochemically the H migration is an endothermic process for both Co(^{i}Pr-MeAMD)$_2$ and Ni(^{i}Pr-MeAMD)$_2$. However, it is much

(16) Lim, B. S.; Rahtu, A.; Park, J. S.; Gordon, R. G. *Inorg. Chem.* **2003**, *42*, 7951.

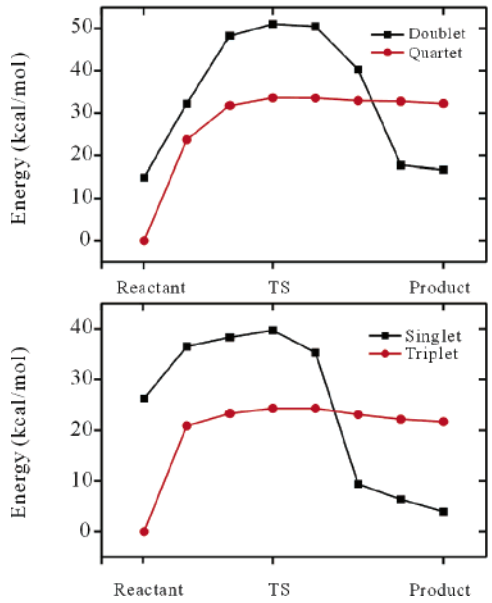

Figure 2. Calculated minimum-energy pathways of both high-spin and low-spin states of Co(^{i}Pr-MeAMD)$_2$ and Ni(^{i}Pr-MeAMD)$_2$.

Table 3. Calculated Reaction Energies (ΔE_r) and Reaction Barriers (E_a) for β-Migration and the Unique Imaginary Frequencies at the Transition States[a]

precursor	ΔE_r (kcal/mol)	E_a (kcal/mol)	imag freq (cm^{-1})
Co(^{i}Pr-MeAMD)$_2$	16.7	33.6	129.8i
Ni(^{i}Pr-MeAMD)$_2$	4.7	24.3	111.5i
Co(^{t}Bu-MeAMD)$_2$	29.2	52.8	309.7i
Ni(^{t}Bu-MeAMD)$_2$	18.5	40.2	295.3i

[a] For M(^{i}Pr-MeAMD)$_2$, the reaction is for β-H migration, and for M(^{i}Bu-MeAMD)$_2$, it is for β-CH_3 migration (M = Ni, Co).

more endothermic for the former than for the latter. In fact, the H migration process for Ni(^{i}Pr-MeAMD)$_2$ is very close to thermoneutral, making the metal atom more available for H attack. Kinetically, the activation barrier of Ni(^{i}Pr-MeAMD)$_2$ is more than 9 kcal/mol lower than that of Co(^{i}Pr-MeAMD)$_2$, implying that the H migration is more rapid on Ni(^{i}Pr-MeAMD)$_2$ than on Co(^{i}Pr-MeAMD)$_2$. The nearly neutral thermochemical energy coupled with a moderate activation barrier makes Ni(^{i}Pr-MeAMD)$_2$ likely to thermally decompose; on the other hand, the unfavorable thermochemical energy coupled with a relatively high activation barrier for Co(^{i}Pr-MeAMD)$_2$ prevents H migration from occurring and thus stabilizes the compound. This result is in excellent agreement with experimental observations.

Qualitatively, the stability difference between Ni(^{i}Pr-MeAMD)$_2$ and Co(^{i}Pr-MeAMD)$_2$ can be understood by analyzing the detailed electronic structure of the transition states and the final products. Our calculations indicate that it is much easier to ionize the d electron in Ni(^{i}Pr-MeAMD)$_2$ than in Co(^{i}Pr-MeAMD)$_2$. The β-H migration leads to the formation of a metal−H bond at the transition state and in the final product, in which the H atom withdraws charges from the metal. As a consequence, more charge transfer from the metal to the H atom occurs in Ni(^{i}Pr-MeAMD)$_2$ than in Co(^{i}Pr-MeAMD)$_2$, resulting in the H−Ni bond being stronger than the H−Co bond. Indeed, the fully optimized structures of the transition states and products exhibit a H−Ni distance much shorter than the H−Co distance. At the transition states, the distances of H−Ni and H−Co are 1.577 and 1.607 Å, respectively, while for the final products, these distances are 1.485 and 1.556 Å.

To enhance the stability of Ni(^{i}Pr-MeAMD)$_2$, we considered utilizing the *tert*-butyl groups to replace the isopropyl groups and performed calculations on CH_3 migration for both Ni(^{t}Bu-MeAMD)$_2$ and Co(^{t}Bu-MeAMD)$_2$. The calculated thermochemical energies and activation barriers are shown in Table 3. As expected, the CH_3 migration processes for both compounds are very endothermic and their barriers are also exceedingly high, indicating great resistance to the migration. Gordon and co-workers prepared the Ni(^{t}Bu-MeAMD)$_2$ compound and found it to be indeed more stable than Ni(^{i}Pr-MeAMD)$_2$ on the basis of thermogravimetric analyses (TGA) of the two precursors.[17] Here we also note that Co(^{t}Bu-MeAMD)$_2$ is much more stable than Ni(^{i}Bu-MeAMD)$_2$.

It should be pointed out that, although our calculations were done only for gas-phase molecules while experiments were performed in solutions, we expect that the qualitative conclusions that can be drawn from the present study remain valid. Nevertheless, it is anticipated that the reaction barriers in all cases could be significantly reduced if the solvation effect is accounted for, which would cause the β-H migration to occur more easily. The computational results presented here provide the upper bound of the activation energies. We are currently pursuing calculations to reevaluate the energetics in relevant solvents that were used in experiments.

In summary, we have performed DFT calculations to examine the relative stabilities of several Co and Ni ALD precursors to β-H or β-CH_3 migration from the chelating ligand to the center metal atom. The calculated precursor structures are in excellent agreement with the available experimental results. The minimum-energy path of the migration process involves two steps: (1) internal rotation along the C1−N1 bond to align the R1 group in the same plane as defined by the M, N1, and C1 atoms and (2) migration of the R1 group from C1 to the metal atom to form the final product. Our results indicate that the migration process is thermochemically endothermic; however, for Ni(^{i}Pr-MeAMD)$_2$ the reaction energy is close to thermoneutral. The relatively moderate activation barrier allows β-H migration for Ni(^{i}Pr-MeAMD)$_2$ to occur readily, leading to instability at the ALD process temperatures. Replacing the H atoms with methyl groups can greatly stabilize the precursors to the β-H migration. The results are consistent with the experimental observations. Understanding the structure−stability relationship is of great importance for design of metal-organic precursors for specific CVD and ALD applications.

Acknowledgment. This project was partially supported by the Research Foundation for Outstanding Young Teachers, China University of Geosciences, Wuhan, People's Republic of China (Grant CUGQNL0519), and Air Products and Chemicals, Inc.

Supporting Information Available: Tables giving the main geometric parameters of the fully optimized reactant, transition-state and final product structures. This material is available free of charge via the Internet at http://pubs.acs.org.

OM060910A

(17) Li, Z.; Lee, D.; Coulter, M.; Gordon, R. G. Unpublished results.